# OBSTACLES AVOIDANCE IN THE FRAME WORK OF PYTHAGOREAN HODOGRAPH BASED PATH PLANNING

M. A. Shah*, A. Tsourdos, P. M. G. Silson, D. James and N. Aouf
*Dept. of Informatics and Sensors, Cranfield University, Cranfield, U.K.*

Keywords: Pythagorean Hodograph, Bending energy, Path Planning, Feasible paths.

Abstract: This paper deals with the problem of obstacle avoidance in the path planning based on Pythagorean Hodograph. The proposed obstacle avoidance approach is based on changing the curvature in case of Pythagorean Hodograph curves. However this may result in an increase in the length of the path. Furthermore in some cases obstacle avoidance by changing the curvature of the path may result not only in an increase in path length but also to a tremendous increase in bending energy. An increase in bending energy of a path as a result of curvature change above certain limit makes the path very difficult or impossible to fly.

## 1 INTRODUCTION

In path planning for UAVs the obstacle avoidance is a common problem. In literature different researcher adopted different ways to solve the problem of obstacle avoidance depending on the context of the problem. (Madhavan at el 2006) and (H. Bruyninckx at el 1997) proposed a solution to avoid the obstacle in case of the Pythagorean Hodograph based path planning for UAVs by manipulating the curvature of the PH path. By changing the curvature of the path an obstacle can be avoided but the path length is increased tremendously as a result. For example figure 1and 2 illustrate this fact:

But sometimes situations arise where obstacles avoidance by changing the curvature of the path results in path of very high bending energy. A path with a very high bending energy is very difficult for UAVs to follow and hence not a feasible path. Figure 3 shows this fact.

Therefore curvature manipulation method can not be solely used for obstacle avoidance in PH based path planning because it is bound to fail for some cases. We need an alternative method for obstacle avoidance which can guarantee feasible (safe and flyable) paths. To elaborate such a method is the subject of this paper.

The rest of the paper is organized as follows: Section 2 describes the problem formulation. Section 3 introduces the Pythagorean Hodograph to generate the initial paths. Section 4 introduces the proposed solution to the problem. Section 5 discusses the simulation results and finally section 6 draws the conclusion.

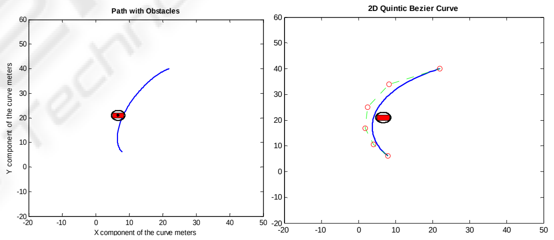


Figure 1: Obstacle avoidance by curvature change.

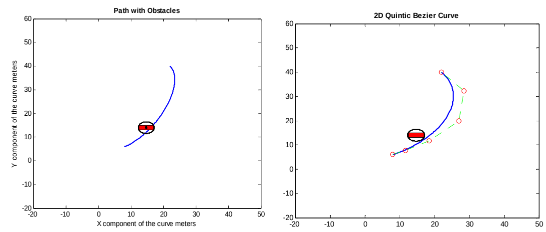


Figure 2: Obstacle avoidance by curvature change.

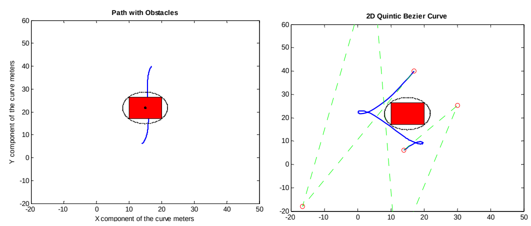


Figure 3: Obstacle avoidance by curvature change.



Shah M., Tsourdos A., M. G. Silson P., James D. and Aouf N. (2010).
OBSTACLES AVOIDANCE IN THE FRAME WORK OF PYTHAGOREAN HODOGRAPH BASED PATH PLANNING..
In *Proceedings of the 7th International Conference on Informatics in Control, Automation and Robotics*, pages 335-339
DOI: 10.5220/0002877803350339

## 2 PROBLEM FORMULATION

A mission is planned to fly a group of unmanned aerial vehicles safely from base B to target T as shown in Figure 4. All vehicles start from the base at the same time. The environment contains stationary and moving obstacles. During the flight, the vehicles will avoid inter-collision and collision with the stationary and moving obstacles. Initially, UAV paths are planned offline by the path planning module (Path Planner) on the basis of the available knowledge about the environment. The UAVs start following these paths, if during the flight any of the UAVs comes across an obstacle, which was not known before then changes are made to the initial path of corresponding UAV to avoid the obstacles while maintaining UAVs cooperation.

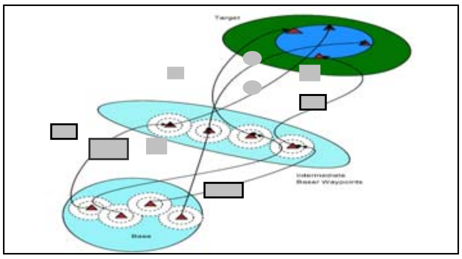

Figure 4: Swarm of UAVs Scenario.

The base and the goal points for each UAV are specified by initial and final poses. Let the starting pose of the $i^{th}$ UAV in the terms of its position and orientation is $P_{si}(x_{si}, y_{si}, z_{si}, \theta_{si})$ and the final pose of the same UAV is $P_{fi}(x_{fi}, y_{fi}, z_{fi}, \theta_{fi})$ then the path of the UAV is defined as a parametric curve *r(t) = [ x(t), y(t), z(t) ]* such that the kinematics and dynamic constraints of the vehicle are satisfied. Mathematically this can be written as:

$$P_{si}(x_{si}, y_{si}, z_{si}, \theta_{si}, \phi_{si}) = r(t_s)$$

$$P_{fi}(x_{fi}, y_{fi}, z_{fi}, \theta_{fi}, \phi_{fi}) = r(t_f)$$

$$P_{si}(x_{si}, y_{si}, z_{si}, \theta_{si}, \phi_{si}) \xrightarrow{r_i(t)} P_{fi}(x_{fi}, y_{fi}, z_{fi}, \theta_{fi}, \phi_{fi})$$

Subjected to:

$$|\kappa_i(t)| \leq \kappa_{\max}$$

$$|\tau_i(t)| \leq \tau_{\max}$$

With curvature $k_i$ and torsion $\tau_i$ for i=1,..,*n* , *n* is the number of cooperating UAVs. In case of obstacle interruption these initial paths are modified such that the modified path is feasible (collision free and flyable). We assume in the developments of our paper that the UAVs are flying at a constant altitude. How we generate these paths is explained in the next section.

## 3 PROPOSED SOLUTION TO THE PROBLEM

The initial trajectories of the UAVs are calculated from known initial and final poses. Therefore the poses play a pivotal rule in generating and modifying these trajectories. For each path there are two poses i.e the initial pose and final pose. The orientation of these poses could be from any of the four quadrants of Cartesian plane. Since there are total of four quadrants, and any two quadrant can be selected at a time for two orientation (one for initial pose and one for final pose), therefore we can have a total of:

$$\binom{4}{2} = \frac{4!}{(4-2)! \times 2!} = 6$$

possible cases. These cases are shown in the figure 5 as a, b, c, d, e and f. There are four more possible cases if the initial and final poses are taken from the same quadrant. These cases are shown in figure 5 as g, h, i and j. The orientations corresponding to initial poses are represented by green arrow and the orientations corresponding to the final poses are represented by red arrow. Referring to the figure 5 below, we have the following cases:

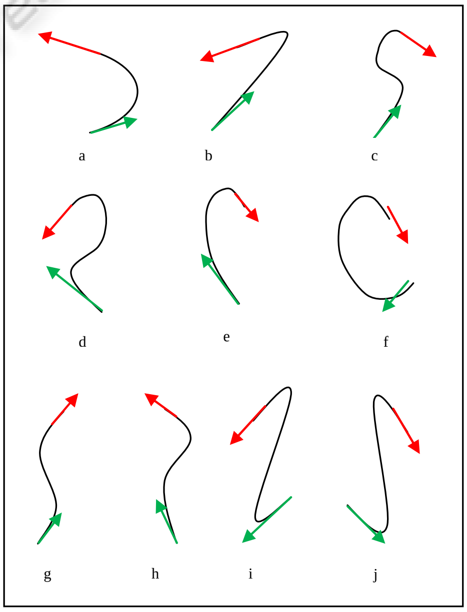


Figure 5: All possible combinations of the initial and final pose taken from four quadrant.

Case a: The initial pose belongs to quadrant 1 and the final pose belongs to quadrant 2. i.e.

$$0 \le \theta_{si} \le \frac{\pi}{2} \text{ and } \frac{\pi}{2} \le \theta_{fi} \le \pi$$

Case b: The initial pose belongs to quadrant 1 and the final pose belongs to quadrant 3:

$$0 \le \theta_{si} \le \frac{\pi}{2} \text{ and } \pi \le \theta_{fi} \le 3\frac{\pi}{2}$$

Case c: The initial pose belongs to quadrant 1 and the final pose belongs to quadrant 4:

$$0 \le \theta_{si} \le \frac{\pi}{2} \text{ and } 3\frac{\pi}{2} \le \theta_{fi} \le 2\pi$$

Case d: The initial pose belongs to quadrant 2 and the final pose belongs to quadrant 3:

$$\frac{\pi}{2} \le \theta_{si} \le \pi \text{ and } \pi \le \theta_{fi} \le 3\frac{\pi}{2}$$

Case e: The initial pose belongs to quadrant 2 and the final pose belongs to quadrant 4:

$$\frac{\pi}{2} \le \theta_{si} \le \pi \text{ and } 3\frac{\pi}{2} \le \theta_{fi} \le 2\pi$$

Case f: The initial pose belongs to quadrant 3 and the final pose belongs to quadrant 4:

$$\pi \le \theta_{si} \le 3\frac{\pi}{2} \text{ and } 3\frac{\pi}{2} \le \theta_{fi} \le \pi$$

Case g: both the initial pose and the final pose belong to quadrant 1: $0 \le \theta_{si}, \theta_{fi} \le \frac{\pi}{2}$

Case h: both the initial pose and the final pose belong to quadrant 2: $\frac{\pi}{2} \le \theta_{si}, \theta_{fi} \le \pi$

Case i: both the initial pose and the final pose belong to quadrant 3: $\pi \le \theta_{si}, \theta_{fi} \le 3\frac{\pi}{2}$

Case j: both the initial pose and the final pose belong to quadrant 4: $3\frac{\pi}{2} \le \theta_{si}, \theta_{fi} \le 2\pi$

Now cases a, b, e and f are safe as shown by figure 1 and figure 2 in the introduction section.

Cases c, d, g, h, i and j have the possibility to give paths of unacceptably higher bending energy when manipulated to avoid obstacles. Therefore they needed some method such that safe and flyable paths are produced.

The method to avoid the obstacle in the case of c, d, g, h, i and j (unsafe cases) comprise of introducing an intermediate waypoint (pose) somewhere between the initial and final pose such that the first and second pose, and, second and third pose can be connected by two PH quintic curves. Each of these two individual PH component becomes like one of the case a, b, e or f.

Since pose is a combination of position and direction, therefore the position and direction of the inserted intermediate pose must be determined. The following paragraphs describe the determination of the position and direction.

## 4.1 Position of the Intermediate Pose

Referring to the figure 6, if $(x_{cen}, y_{cen})$ are the coordinates of the centre of the obstacle, $r_d$ is the radius of the circle enclosing the obstacle, then the coordinates of the points of the circle enclosing the obstacle are (x, y) given by the following equations:

$$x = x_{cen} + r_d \cos\theta$$

$$y = y_{cen} + r_d \sin\theta$$

Where $\theta \in [0 \ \ 2\pi]$

The position $(x_{iwp}, y_{iwp})$ corresponding to the new waypoint is given by:

$$x_{iwp} = d_{saf} + x_{cn} + r_d \cos\xi$$

$$y_{iwp} = d_{saf} + y_{cn} + r_d \sin\xi$$

$\xi = \frac{\pi}{2}$, if the UAV is approaching from the bottom of the obstacle.

$\xi = \pi$ , if the UAV is approaching from the right.

$\xi = 3\frac{\pi}{2}$ ,if the UAV is approaching from the top.

$\xi = 0$ ,if the UAV is approaching from the left. $d_{saf}$ is the safety distance.

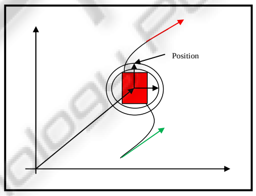


Figure 6: Position specification of the intermediate waypoint.

## 4.2 Direction of the Intermediate Pose

The intermediate waypoint is inserted between the initial and final poses. The direction of the intermediate waypoint $\theta_{iwp}$ is such that when the two consecutive poses are connected via PH quintic in case of c, d, g, h, i and j each individual PH segment becomes like one of the cases a, b, d or e. We consider each individual case separately.

Case g, i: If both the directions of initial and final poses belong to quadrant 1 or quadrant 3 then the

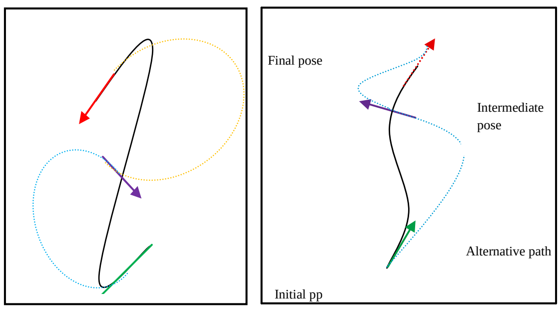


Figure 7: Direction of intermediate waypoint for cases g and i.

direction of intermediate pose is $\theta_{iwp} = \theta_{si} + \frac{\pi}{2}$

Case h, j: If both the directions of initial and final poses belong to quadrant 2 or quadrant 4 then the direction of intermediate pose is $\theta_{iwp} = \theta_{si} - \frac{\pi}{2}$

Case c: If the directions of initial pose belong to quadrant 1 and that of final poses belong to quadrant 4 then the direction of intermediate pose is

$$\theta_{iwp} = \theta_{si} + \frac{\pi}{2}$$

Case c inverted: If the directions of initial pose belong to quadrant 4 and that of final poses belong to quadrant 1 then the direction of intermediate pose is $\theta_{iwp} = \theta_{si} - \frac{\pi}{2}$

This is shown in figure 9.

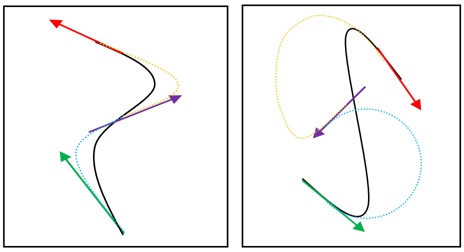

Figure 8: Direction of intermediate waypoint for cases h and j.

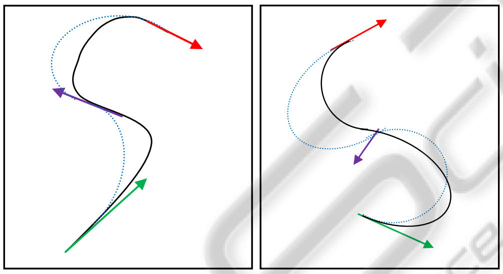

Figure 9: Direction of intermediate waypoint for cases c and c inverted.

Case d: If the directions of initial pose belong to quadrant 2 and that of final poses belong to quadrant 3 then the direction of intermediate pose is: $\theta_{iwp} = \theta_{si} - \frac{\pi}{2}$

Case d inverted: If the directions of initial pose belong to quadrant 3 and that of final poses belong to quadrant 2 then the direction of intermediate pose is $\theta_{iwp} = \theta_{si} + \frac{\pi}{2}$

## 4 SIMULATION RESULTS

The simulation results are obtained y taking only one case in which the direction of initial and final poses belong to quadrant 1. The method can be tested for the rest of cases. The two methods (the curvature manipulation method and the proposed method) were simulated by taking the initial pose (14, 6, 60$^o$) and final pose (17, 40, 60$^o$). The following results were obtained.

Figure 11 shows the path and the obstacle (red rectangle).

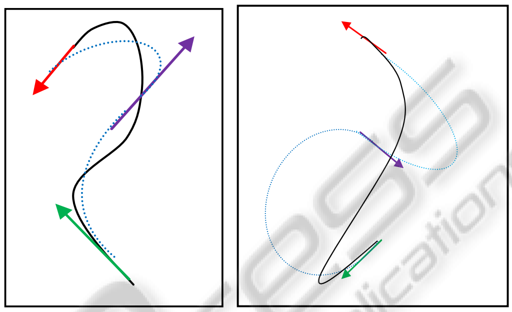

Figure 10: Direction of intermediate waypoint for cases d and d inverted.

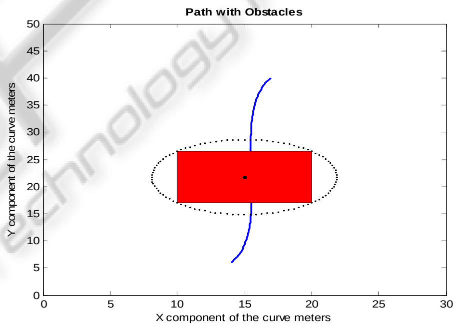


Figure 11: The path with the obstacle.

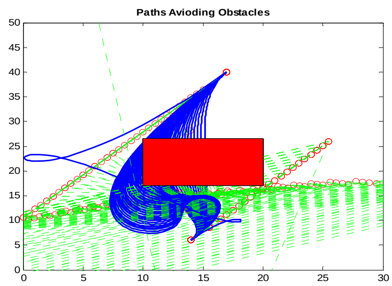


Figure 12: The path with different stages of curvature manipulation to avoid the obstacle.

When the curvature manipulation method was applied to avoid the obstacle (figure 12), the result was a path with an unacceptable bending energy as shown in the figure 13. The path shown in the figure 13 is not a flyable path because its high bending energy makes it difficult to obey the dynamic constraints. If we try to impose the dynamic constraints then its length will be increased tremendously. The proposed method can offer a remedy to this problem. The proposed method is applied to insert an intermediate pose between the initial and final pose. Then the three poses were connected by the application of Pythagorean Hodograph curves such that the individual curves comply with the afore mentioned safe cases.

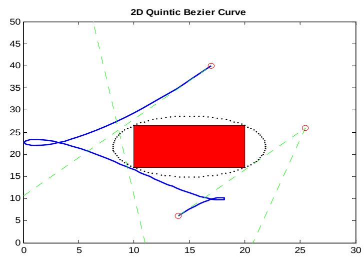


Figure 13: The final obstace free path with very high bending energy.

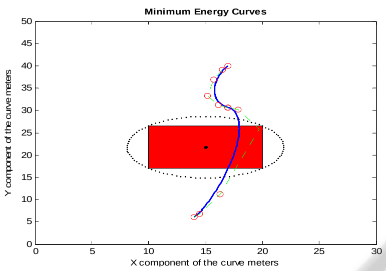


Figure 14: The path with same initial and final poses resulted from the proposed method.

The result is shown in the figure 14. Figure 15 show the same path after imposing the dynamic constraints. Figure 16 shows the iterative process to avoid the obstacle. Figure 17 shows the final obstacle free path. The path shown in figure 17 obeys the dynamic constraints. The binding energy is much lower compared to the path achieved with the curvature manipulation method. The length of the path is optimal as well.

## 5 CONCLUSIONS

The curvature manipulation method fails to give feasible paths if the angle of the initial pose and final pose in the first quadrant is increased above $60^o$ and $55^o$ on the upper side and decreased below $40^o$ and 30 on the lower side. Therefore the operational angle band of the method is very narrow which makes it unsuitable for practical purposes. The proposed method can accommodate poses with all the angles. More over the path length of the resultant path is optimal.

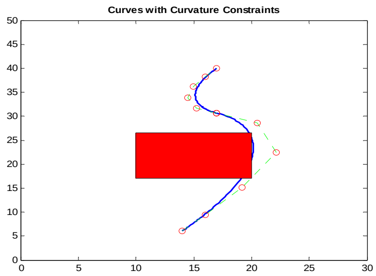


Figure 15: The path with curvature constraint.

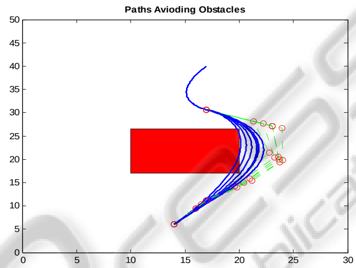


Figure 16: The curvature manipulation of the path to avoid the obstacle.

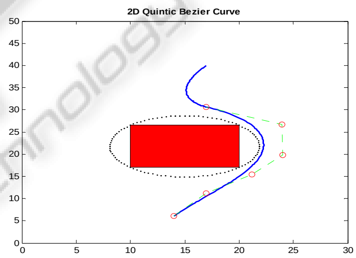


Figure 17: The obstacle free path with reasonable bending energy and reasonable path length.

## ACKNOWLEDGEMENTS

This research was sponsored by Engineering Physical Science Research Council (EPSRC) and British Aerospace (BAE Systems). Support is gratefully acknowledged and appreciated by the authors.

## REFERENCES

S. Madhavan, A. Tsourdos, B. White. "A Solution to Simultaneous Arrival of Multiple UAVs using Pythagorean Hodograph" American Control Conference, Minnesota USA, June 2006.

H. Bruyninckx, D. Reynaerts, "Path planning for mobile and hyper redundant robots using Pythagorean hodograph curves", In 8th International Conference on Advanced Robotics, ICAR, 97 pages 595-600, 1997.